

Jean Martial Mari¹, Christian Cachard²

¹*Medical Vision Laboratory, Engineering Science, University of Oxford,
Parks Road Oxford, United Kingdom, e-mail: mari@robots.ox.ac.uk*

²*CREATIS, Université de Lyon, Université Lyon 1, CNRS UMR5220, INSERM U630, Bat.
Blaise Pascal, INSA-Lyon, 7 avenue Jean Capelle, F69621 VILLEURBANNE cedex, France
e-mail: christian.cachard@creatis.univ-lyon1.fr*

Acquire real-time RF digital ultrasound data from a commercial scanner

Received 06.12.2006, published 24.01.2007

Although new ultrasound signal processing can be designed from simulation data or recorded data, the development and prototyping of new medical ultrasound imaging tools is essentially based on processing the radio frequency (RF) data, which is the signal generated by the ultrasound probe. Unfortunately, the diversity and technological level of knowledge required for implementing a whole ultrasound scanner from scratches are usually found in the companies that manufacture such engines. The implementation of the new methods in the laboratories is then tributary to the interest and good will of those companies, and the lack of such experience makes technological transfers even more difficult. But another approach of the problem can be chosen: the direct acquisition of the real time RF data in a commercial scanner. This approach takes advantage of the high technological level of the transceiver of the commercial ultrasound scanners and frees the researcher from the post processing applied by each company. The side effects of such approach are resumed to the difficulty of interfering with the scanner's electronic systems, but this problem is simplified by the high technological level of the modern engines. Indeed, their digital conception makes the electronic signals easier to understand and the manual operations safer, and the impact of an unfortunate manipulation is essentially reduced to a distortion of the scanner's display. In this paper, the general approach of RF derivation in a commercial digital scanner is exposed. Then it is demonstrated on a commercial scanner, the Kretztechnic 530D, equipped with a volumic probe. This system allowed us to implement one of our current subjects of research, that is the Parallel Integral Projection for the localization of a micro needle in soft tissues, and to conclude on its performances on real data, including a minimum gain of 5.

INTRODUCTION

Ultrasound images quality has improved with the technological evolution of probes and the development of harmonic imaging [1]. New fields of application appeared and the radio frequency (RF) signal has become fundamental for the development of new imaging techniques and has improved analysis and diagnosis in medical imaging. The RF signal is the scattered signal received by the ultrasound scanner's probe. It thus contains all the information on the propagation of the acoustic waves and their interactions with the scanned

medium [2]. The electric signal delivered by the ultrasound probe is a filtered version, in the bandwidth of the probe, of the acoustic pressure scattered by the medium in response to the transmitted pressure field. The development and improvement of imaging techniques in order to establish the intrinsic properties of the medium or other parameters requires the use of the whole information available in this signal.

The image displayed in an ultrasound scanner screen, known as the B mode (or envelope) image and used for medical diagnosis, contains less information than the original one received by the probe. The ultrasound backscattered signal is displayed after many processing steps which are time-gain compensation, filtering, rectification and log-compression. For a sectorial probe, the resulting image is interpolated from the raw data in order to convert the polar coordinates acquired signal into the cartesian coordinates of the screen. Moreover every scanner performs these operations in its proper manner. A typical implementation of these signal processing steps is detailed later in part 3.2. Because of the specificity of the processing on each scanner, images displayed on the screen are difficult to compare from one machine to another. In practice, the B mode image is a representation of the envelope amplitude of the backscattered signal which, once processed, has lost its proportionality to the medium's pressure response. The loss of information due to these processing is critical to take full advantage of the received signal in terms of signal processing and automatic diagnosis. As a consequence, the elaboration of new imaging techniques, and the corresponding medical tool, which require the real time RF signal, is delayed. Indeed new signal processing methods can be performed by the research teams, but their implementation on a prototyped medical tool depends on the interest shown by the scanners manufacturer and the commercial choices they make.

For example, elastography [3, 4] which is an in-development imaging technique, processes RF signals to investigate the deformation behavior of soft biological tissues under load. This method computes a strain map from pairs of RF signals acquired at two different pressure levels by tracking the variation within signals induced by the load application. On the same way, contrast imaging is not as efficient in B mode as it could be. Processing the RF samples is required to extract typical parameters of the contrast agent [1, 5–7]. Another example is the visualization of micro surgical tools introduced inside the body during the medical intervention. Due to the small sizes, inferior or same order as the wavelength, and mechanical properties of these tools, their manipulation requires the development of new imaging techniques to accurately detect and localize them. But the usual post processing performed on the RF signals, like log-compression or rectification makes this problem difficult to solve. New algorithms have been developed [8–10] and require the RF signal in order to take full advantage of the information available in it. Few manufacturers (ATL, Vigmed, GE, and Siemens) propose some ultrasound scanners that deliver the RF signal, but most of them are not available without a specific research agreement. Vigmed sells a scanner that allows recording RF signals on the scanner memory in IQ mode. The files need then to be transferred to a workstation in order to be processed with dedicated software. However the RF signal is available only with some specific probes, most of them working at low frequencies (inferior to 5 MHz). Those kinds of equipment are also available with the Logic scanners of General

Electrics Medical System Company and its so-called TrueAcces technology, with the Technos family from Esaote and their VPAN storing system develop by Ultrasound Network Architecture, and with the Sonoline Elegra from Siemens. The signals are stored in the scanner and have to be transferred on a workstation and processed off line.

Some research groups have developed their own dedicated high frequencies scanners that deliver the RF signal. In these cases, the probe is generally made of a single element mechanically moved to perform an image. The Dermcup 2020 (Ultrasons Technologies, Tours, France) is a high resolution research scanner working at 20 MHz and dedicated to researches on skin [11]. VisualSonics (Toronto, Canada) made a 40 MHz scanner, the Vevo 660, for small animals imaging [12]. The Femina [13] and Rasmus [14] systems have been developed for beamforming studies. Other groups develop their own research scanner [5, 15], but this requires lots of knowledge and strong investments of money and time, on topics that are not directly related to the research goal. In reaction to these needs in the ultrasonic research field, Ultrasonix Medical Corporation with the ES500RP, and Analogics, with the Casablanca Engine, are offering new tools which have lots of functionalities; but these are provided with specific probes and systems, and the RF signal is not available for processing on other machines in real time, but is stored locally.

In this paper, we describe a general approach based on our experiment to transform a commercial scanner into a RF research tool working in real time whatever the connected probe. The paper is organized as follows: section 2 presents the general approach to transform most of the scanners currently commercialized, followed by example based on a dedicated implementation on a Kretztechnic Voluson 530D in section 3. Section 4 gives the steps of the signal processing leading to the B mode image, and section 5 gives an example of direct processing of the RF signal in comparison to B mode image processing, and the resulting improvement on the resolution of needle localization.

1. GENERAL APPROACH

1.1. Beamforming and synchronization signals

The ultrasound probe is composed of several of piezoelectric elements (usually 64, 128 or more) working alternatively in transmission and reception [16]. Delays are applied individually to each active element to focus and steer the ultrasound beam. The RF signal, of a multi element ultrasound probe, is achieved by the beamformer which performs a linear combination of the signals received by each element. After some post processing, the RF signal is displayed as a gray level image. So, the RF signal coding ultrasound backscattered by the tissue should be captured just after the beamformer, before these post processing. Another way is to acquire the element signals separately [5] and to perform a custom beamforming on a dedicated workstation, but this would require a multi channel acquisition system which is already part of the scanner.

In order to take advantage of the raw data, the line, frame and volume (in 3D mode) synchronization signals have to be captured. These three synchronization signals give the beginning of each line, frame and volume respectively, and allow parsing the data. Typically, the frequency of the line synchronization signal, or pulse repetition frequency (PRF), is in the

range of 5 to 10 kHz, depending on the depth of the scanned area. The frequency of the frame synchronization signal, or frame rate, varies usually from 15 up to 80 Hz. On a 3D scanner, the volume synchronization signal is not periodic, as most of the scanners perform single volume imaging. The raw data are sampled at a frequency which is about 4 times the highest frequency of the probe's bandwidth, which is typically in tens of MHz. The sample frequency is elaborated from the clock signal which rates all operations in a digital scanner. So four control signals (line, frame and volume synchronizations and clock) have to be captured and transferred to use accurately the raw data. The samples are commonly coded on 12 or 16 bits.

1.2. RF bus and synchronization signals identification

In a scanner, the first step to bypass the RF signal is to localize the RF bus and the synchronization signals. The common organization of a scanner in electronic boards, each dedicated to one or more specific post processing, eases this task. Furthermore, the synchronization signals keep along the RF bus during their transmissions from the probe to the final image computation, making their localizations easier. The beamformer can be found as connected (Figure 1) to the transmission-reception block (TX/RX block) which has to be systematically screened from the other boards. In entrance of the beamformer, single electrical lines coming from the probe and that are a multiple of the active element's number (64, 128, ...) are delayed and summed.

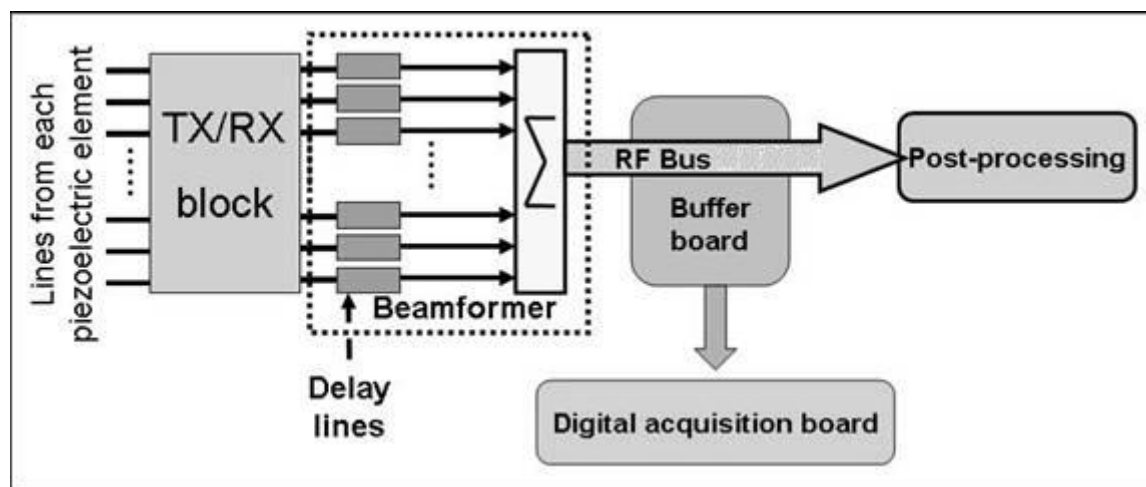


Figure 1. Synoptic of a digital scanner reception and RF signal elaboration block equipped with a buffer board

For those reasons, the beamformer is also typically recognizable by the delay lines and summation circuits that are implemented many times in parallel. The others boards, usually dedicated to more elaborate functions, should have more varied circuits and micro-chips, and should be located more distant to the TR/RX block. The RF bus is the beamformer output, located directly after the summation circuit.

1.3. Samples acquisition

As the RF bus and synchronization signals have been localized, they have to be picked up without disturbance. So, these signals should be buffered for bypass. After, this bypassing, a digital acquisition board inserted in a workstation has to be used to transfer the samples to a memory. The acquisition board should be able to work at the RF bus frequency, to synchronize on an external clock and to acquire large data words. A critical parameter is the memory size of the acquisition board, which should allow the acquisition of at least a whole image and at best a whole volume. The number of samples per image is the ratio of the sampling frequency over the frame rate. Finally, the samples of RF lines are available in a vector stored in the acquisition board in real time for all the future custom processing. However the transfer rate between the acquisition board and the workstation fixes the speed limit of data availability for signal or image processing. Therefore attention must be paid on the choice of the digital acquisition board.

2. EXAMPLE WITH A KRETZ 530D

An RF research tool has been implemented under this general approach with a Kretztechnik 530D. This scanner offers a particularly interesting configuration since in addition of allowing volume imaging and the use of various kinds of probes, it presents a clear organization of the boards and data flows.

2.1. Organization of the engine

The engine is organized in two shielded blocks, each with a specific task: the upper one, or ‘GET module’, contains the transceiver and beamformer units, and the lower one, or ‘GAA module’, contains the interface engine and the post processing systems. The ‘GET’ module is composed, as illustrated on Figure 2, of several parallel electronic boards of 320 mm per 254 mm, plugged in a motherboard that distributes the power and different signals between the daughter boards. The connection between daughter and mother boards is performed with METRAL® modules, the male part connected to the motherboard and the daughter part to the daughter boards.

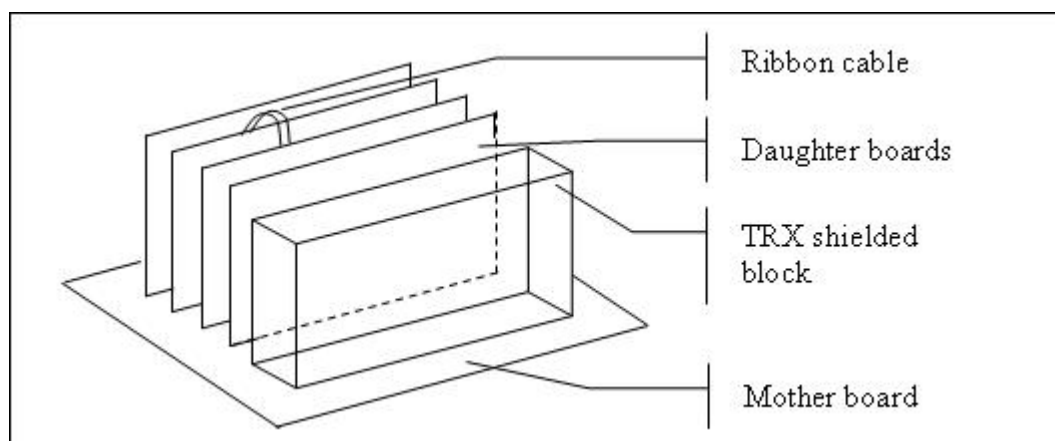


Figure 2. Board organization of the GET module in the Kretztechnik 530D

The RF data are flowing from the probe to the display unit. Such a display requires the signal to be formed and modified during many steps. As each board implements a specific task, they need to transfer the samples from one to another. This is how the samples were identified on two ribbon cables between two daughter boards, as shown on Figure 3.

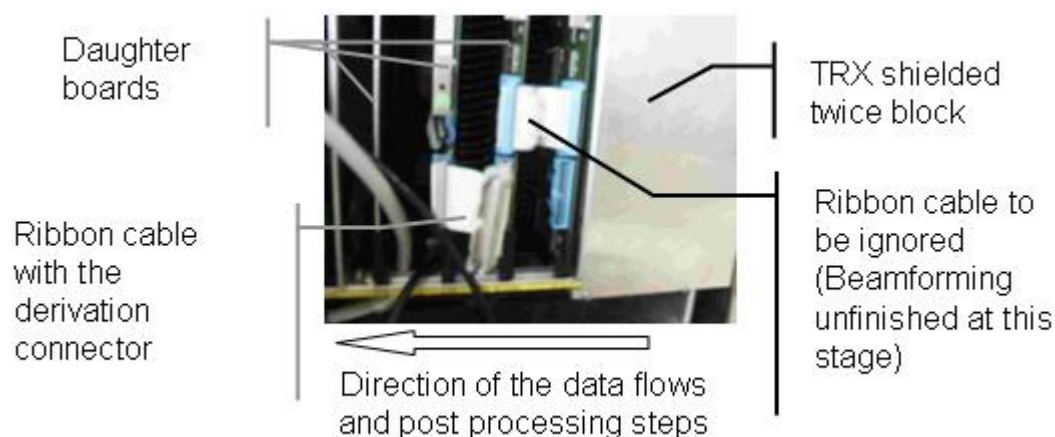


Figure 3. Picture of the boards of the GET block and of the RF transmission ribbon cable

2.2. Localization of the main signals

The RF data are transferred between two boards on a ribbon cable, just after the beamforming, which make the electrical derivation much easier. The final tool delivers the RF samples and synchronization signals for any of the ultrasound probe of the scanner, making it probe independent. The RF samples are transferred through another ribbon cable by 16 bits words at a 27 MHz sampling frequency. Synchronization signals are also required so as to correctly parse the data in lines and images. These signals have a frequency that depends, in a limited range, on the user's parameterization of the scanner. The line signal frequency (PRF) varies around 5 kHz and the frame rate (FR) around 30 Hz. So the average image size is around 1.5 MB (Mega Bytes). The clock signal is picked up directly on the bus buffer and is connected to the acquisition board in order to synchronize the recording. The line and image synchronization signals were searched through a completed analysis of the signal on the free METRAL[®] connectors of the free slot of the motherboard. They were found available as detailed on Figure 4. The volume synchronization signal was found located on the connector of another board, on pin BYB/A03-C07 (the letter-number reference is found on the board). It is bypassed with a specially shielded cable to an unused wire of the available slot of the mother board.

An example of visualization of synchronization signals is given in section 3.1.

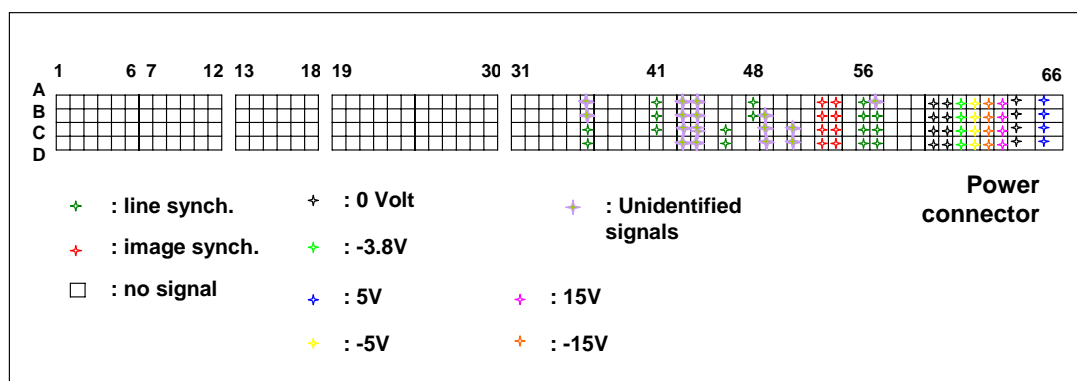


Figure 4. Signals available on the METRAL[®] free connectors on the mother board

2.3. Bypass

A dedicated buffer board was developed and inserted in the available slot. This empty slot permits to install a dynamic derivation board supplied by the scanner, which avoids installing a specific power supply.

So the onboard buffers are powered directly by the supply connectors of the motherboard, the available power being far larger than the consumption of the buffers. A Philips[®] ABT 740 three states auto synchronized buffer working up to 30 MHz on 8 bits was chosen. The auto synchronization simplifies the board and avoids using the 27 MHz sinusoid signal onboard. At least three of them are necessary to buffer the 16 bits data and the four synchronization signals.

Such a board must be shielded as much as possible with large ground planes. It is also advised to use one cable out of two on the ribbon cable usually used to transfer the sample to the acquisition board, and to connect those shielding cables to the ground on both ends to ensure proper shielding. A synoptic of the electrical circuits is given in Figure 5.

Once the samples are properly bypassed, they are transferred through a ribbon cable to a slot created on the GET module, and through a second ribbon cable to the workstation.

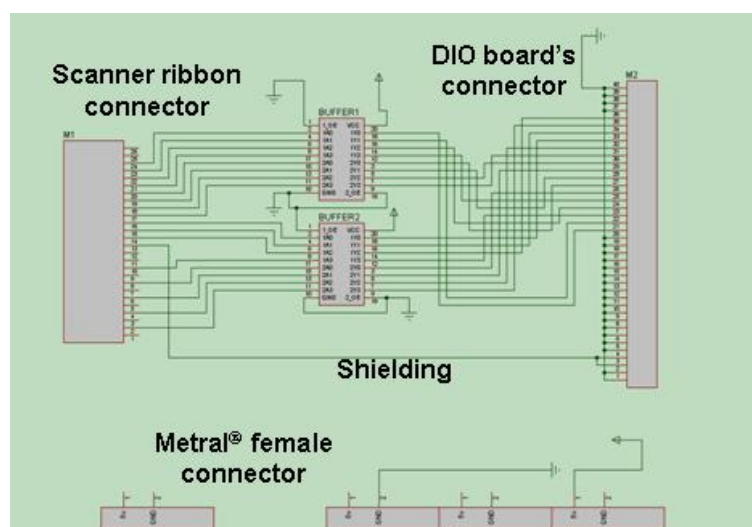


Figure 5.

Synoptic of the connection of the data buffers.
The signals are reorganized

2.4. Acquisition

The DIO (Digital Input-Output) board inside the workstation can then receive all the required signals to reconstruct the ultrasound data. A digital acquisition board, SPECTRUM[®] DIO32 was plugged on a workstation to acquire the data samples. This board is a 32 input bits and is thus able to acquire the 16 data bits and the 3 synchronization signals. The board works up to 100 MHz and synchronizes the acquisition on an external clock. This acquisition board has a 128 MB memory, corresponding to 32 mega words of 4 bytes samples. Software, Sbench 5, provided with the board, eases the data acquisition by offering online visualization of the acquired signals. The drivers of the SPECTRUM[®] DIO 32 are available in Matlab[®] and C languages. One function is dedicated to the data transfer to the workstation memory.

The Matlab[®] drivers and commands are used to configure the acquisition. The whole volume acquisition is triggered by the volume synchronization signal and the board is filling its memory with the RF samples and synchronization signals.

Typically, a polar volume as the one in Figure 6 of 40° per 40° is composed of 53 frames, each composed of 71 RF lines of 1300 samples. Once recorded, the data need to be parsed before the RF image becomes available.

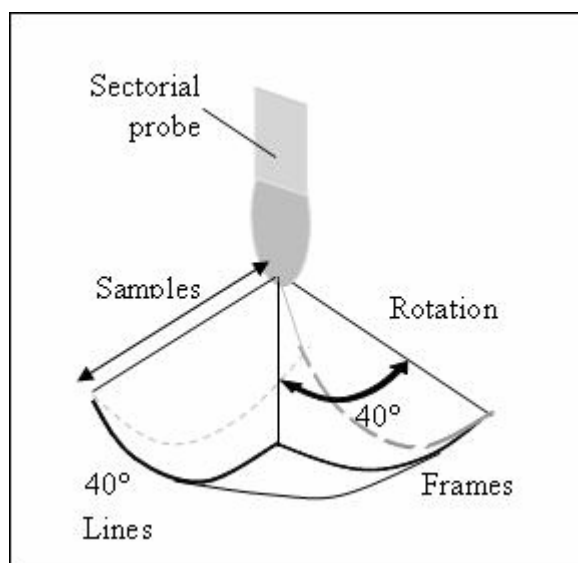


Figure 6. Polar volume acquisition with a sectorial probe (here is an example for a 40° by 40° acquisition volume)

3. PROCESSING A B-MODE IMAGE

Once the samples are recorded in the workstation's memory, they are available for testing new algorithms in order to improve the B mode image or to superimpose new information on it. In order to mimic the B mode image displayed by the scanner, the RF signal has to be analyzed. The processing steps are detailed below.

3.1. Parsing the raw data

The samples are stored in the workstation memory as a raw data vector. It has to be parsed according to the synchronization signals. The timing of the volume, frame and line signals allows performing a simple parsing of the samples, as shown in Figure 7. Cutting up the raw data leads to a set of RF lines stored as 3D arrays with frames, lines and samples. Figure 8 shows a part of one parsed and band-pass filtered RF line. The samples are coded in two's complement.

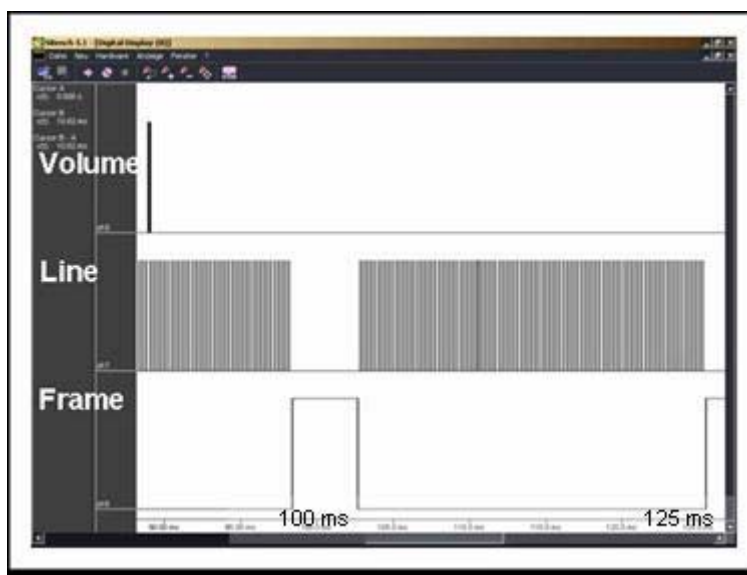


Figure 7. Synchronization signals (volume, frame, line) of the Kretz 530 D for parsing the raw RF data acquired by the Spectrum DIO32 board and visualized by the Sbench5 software

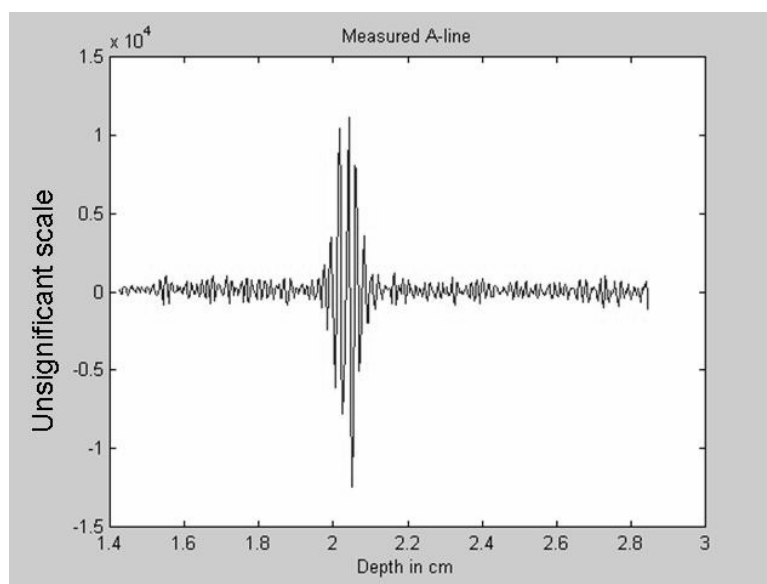


Figure 8. Example of a RF line

3.2. B mode image construction

Once the lines are stored in the workstation's memory as 3D arrays, it might be useful to display the B mode image as the scanner does it. The scanner performs some signal processing to make the data fit the human eye perception and distinguish tissues with close properties. Typically, a band-pass filter, a rectification, a logarithmic compression and a low pass filter are applied to the samples. Figure 9 presents post processing steps for a single line (central column) and the resulting image at each step (right column). Figure 9a gives the RF data issued from the beamformer without any post processing. As no detail is observable, this figure shows that the signal cannot be displayed directly and should be processed in order to make it suitable to the human eye's perception. Figure 9-b illustrates the results from filtering the RF signals in the bandwidth of the probe (2 to 9 MHz), removing the noise induced by the reception bloc and digitalization. Figure 9-c gives the image after detecting the envelope of the filtered RF signal. This operation removes the frequential information from the RF signal and makes it useless to many algorithms like the ones for elastography [3, 4] or contrast agent imaging [1]. Figure 9-d shows the log compression step. This step is required to visualize both weak and strong backscattered echoes (Figure 9-c and Figure 9-d), but is not suitable to process highly echogeneous structures like surgical tools. The log compression reduces the signal's dynamic, i.e. the large and small values are reduced into a smaller range. The signals backscattered by the tool are then merged with the ones backscattered by the surrounding tissue.

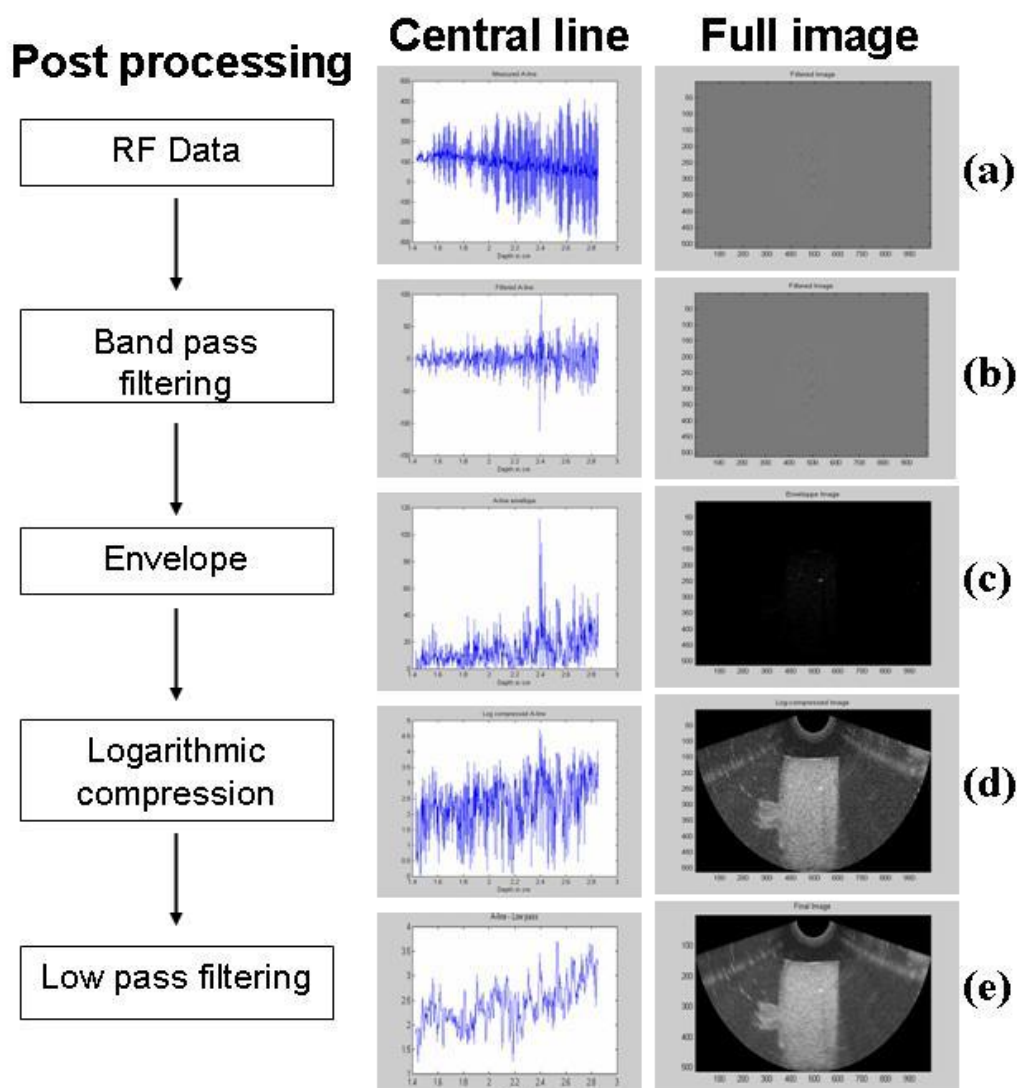


Figure 9. Post processing steps of the elaboration of the typical B mode image. Central column presents the center line of the same frame for different post processing steps. The right column gives the full image for each step. Comparison of image (a) and (d) shows that some post processing is required to display both small and strong signal amplitude, i.e. an image that fits the eye sensibility

Finally these post processing, especially the envelope calculation and log compression, are leading to the conclusion that the signal displayed by the scanner is very different from the one acquired by the system and that the access to the RF signal is essential to develop advanced processing.

4. EXAMPLE OF DIRECT PROCESSING OF THE RF RAW DATA

The accurate localization of a needle inside biological tissues from an ultrasonic volume of data is not an easy task, even if this kind of target is commonly considered as strongly scattering. The main difficulties are due [7–9] to the specificity of the 3D texture of ultrasound data and to the varying amplitude of the echoes scattered along the target. When the needle is scanned at normal incidence of the transmitted beam, the amplitude of the scattered field is strong and a simple threshold leads to an immediate detection and visualization of the tool. But this incident position is rare and does not occur in the common cases, particularly with the growing use of sectorial probes. Those probes steer the beam in order to perform a sectorial acquisition, which implies in most cases that the beam's incidence angle changes along the needle and provide varying amplitude of the scattered field. The needle can sometimes be clearly seen, but is usually difficult to distinguish from the surrounding tissues. Moreover the ultrasound data exhibit a special texture with an azimuthally and transversally orientation due to the non ideal size of the beam's resolution cell. When using local orientation or differentiation operators, the results are mostly oriented azimuthally and transversally, with a high level of noise.

These problems can be solved by the implementation of a global operator like the Parallel Integral Projection (PIP) [7–9]. This operation consists in accumulating the volume samples values normally to a projection plane, and to calculate this integral projection along all directions. It is similar the X Ray tomography computing with a parallel source. When the image plane of the needle is normal to the accumulation plane, then a maximum is observed, corresponding to the highest probability of presence of the target. This transform is particularly robust and allows localizing the needle even when this latter is hardly seen in the acquired data volumes.

But this estimation remains difficult to perform when the data volume is composed of a set of B mode images. The operations performed in order to transform the RF lines into a 2D image alter the signal and require an interpolation of the unknown data between two lines, which acts like a low pass filter. When imaging a micro tool such as a 150 μm diameter tungsten needle, the target image size can be up to 20 times bigger than the target itself. The solution is to measure and process directly the RF data without any post processing after the beamformer. We implemented the PIP in order to process RF polar data; this makes it suitable to process any kind of ultrasound data. The parameter chosen to estimate the accuracy of the localization is the apparent diameter at -3 dB on the accumulation plane computed for the maximum of accumulation. Figure 10 (a) and (b) illustrate the benefit on simulated data, with (a) the result from B mode data and (b) the result on its original RF data.

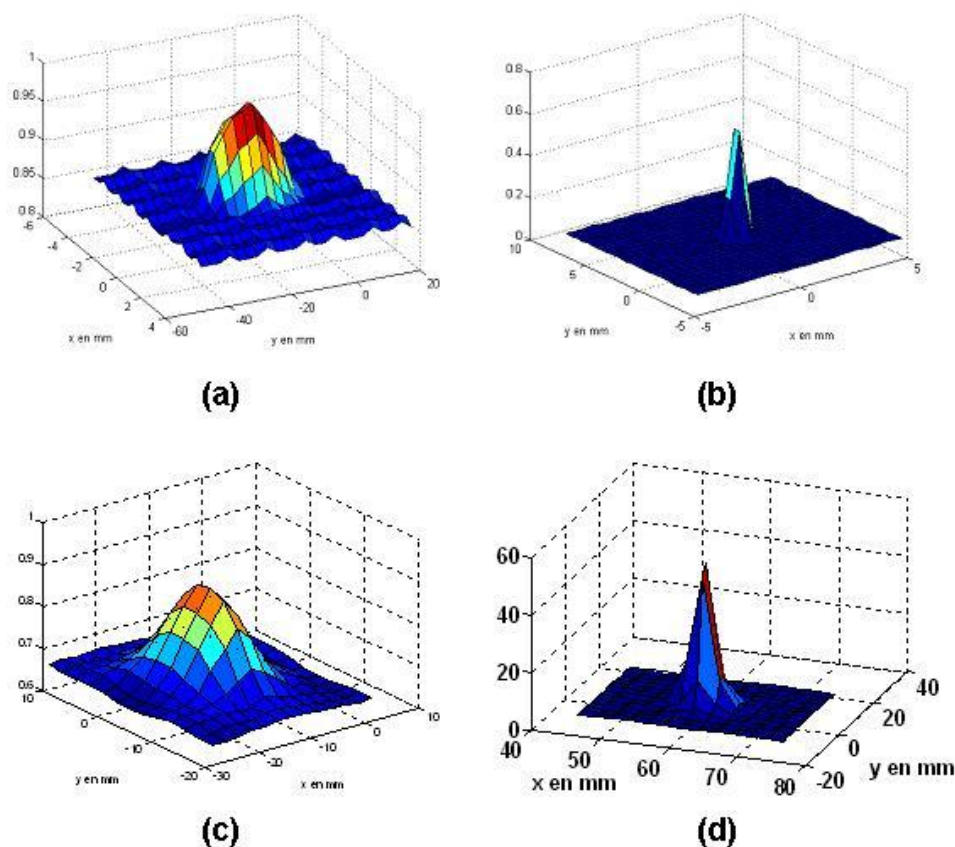


Figure 10. Maximum accumulation plane of the PIP applied on B mode data (a, c) and RF data (b, d) with simulated data (a, b) and real data (c, d) acquired from a Cryogel phantom crossed by a $\varnothing 150\ \mu\text{m}$ tungsten needle. The diameter at $-3\ \text{dB}$ is an estimator of the needle diameter. Diameter is at least 5 times smaller in (b, d) cases than (a, c) respectively, thanks to the direct computation of RF lines

Figure 10 (c) and (d) illustrate the benefit on real data measured on a gelatin phantom, with (c) the result on mode B reconstructed data and (d) the result for the original RF data. The real data were acquired on a gelatin tissue mimicking phantom crossed by a $150\ \mu\text{m}$ diameter tungsten electrode. The data were directly transferred on the workstation that processed them and, unfortunately, it is this latter step that slows down drastically the processing speed. But improving the workstation speed is technically the easiest part of the job. However, results show (Figure 10) that processing only radial data and not a cartesian 2D gray level image reduces the apparent diameter of the target. The results given in Figure 10 are computed, in each case, on the envelope of the RF data and the corresponding B mode volume. Results on simulated data show that the use of RF data improves by a factor of at least 5 and up to 12 the apparent diameter of the target. Results on real data show an improvement by a factor of at least 5 and up to 11. The computation time between grey level volume and RF volume was reduced at least by 15, a single accumulation of a $60 \times 80 \times 1000$ (samples) volume with non optimized code under Matlab[®] software taking about 5 seconds on a 3 GHz Pentium PC with 1 GB of memory.

The PIP was performed on full RF data of a volume acquired over an ex-vivo pig liver crossed by a 150 μm in diameter tungsten needle. The image of the maximum accumulation plane is given in Figure 11. In this figure several picks can be observed, that would not appear separated in the accumulation plane was performed on gray level images. Such peaks offers more information in the accumulation plane and increase the resolution of the localization; here typically by a factor of 3.

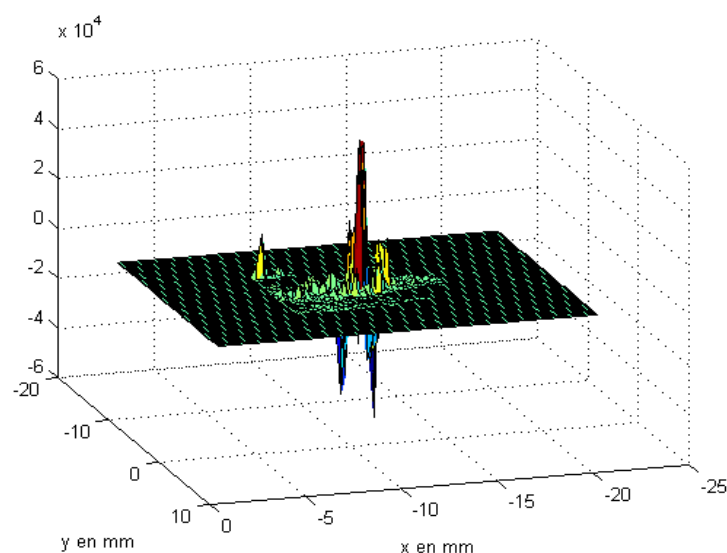


Figure 11. Maximum accumulation plane for a volume over a 150 μm in diameter tungsten needle into pig liver; the PIP is performed after proper data selection

DISCUSSION

The approach exposed previously might seem complicated and hazardous given the complexity of the recent ultrasound engines. Moreover, it could be considered that each model may have a different organization and technology, but since no full integration of such systems has been performed on a single chip, the materials available, the effective technologies and the technical fashions are limiting this complexity. So all ultrasound scanners will, with limited changes, follow the same principles and present the same organization. In fact the more problematic aspect of the difference between brands will rely on the processing applied by the circuits. Indeed these processing are encoded in the memories of the on board chips, and is the most difficult part to retrieve, if ever required. For example, the function applied for Time Gain Compensation (TGC) is usually built in and unknown if not released by the manufacturer. It should be noted that the signal delivered by the RF scanner presented here is bypassed after the engine's TGC is applied. In the same time, no engine, to our knowledge, is offering RF files without TGC. The negative point is that some blind amplification is applied to the acquired signal, making it less interesting for automatic TGC model testing; but, as on the Casa Engine, this blind TGC can be removed.

The positive aspect is that the acquired signal is available with the settings applied to the engine, so the data to be processed correspond to the one displayed on the screen of the scanner, with no bad surprise when plotting previously acquired signals. But the greater task to be performed is the localization of the signals inside the engine. Some may be localized more easily, like the clock and the line and frame synchronization signals, but the volume synchronization might be more problematic because it is not. Finally, it is possible that manufacturing companies will allow more confident relationship with laboratories; but the increase number of private funding of research would probably only slow down such process, as it enforces financial interests; on another hand it can be considered that future scanners from dedicated companies may allow real time implementation of RF processing. However the approach exposed here would not be completely obsolete, as it also allows to convert and use older machines that were equipped at great costs of efficient components and functions, and that do not offer the RF signal yet for up to date research, and that such a task is keeping the ultrasound researchers in the technical loop and teaches the technical basis of every ultrasonic system. As exposed previously, the developed scanner allowed our team to implement the PIP on real data and to quantify the resolution improvement. The post processing steps of the ultrasound engines exposed previously and the PIP results clearly suggest that further processing of ultrasonic signals should be performed directly on the RF data and not on the gray level displayed image.

CONCLUSIONS

A general method to develop a real time RF ultrasound research scanner based on a commercial one has been exposed, with an example of implementation given on a Kretztechnic Voluson 530D. The result is a multi-probe real-time digital scanner allowing the acquisition of images and volumes on a workstation. We showed that the post-processing performed on commercial scanners is dedicated to fit the operator's eye, but it is not suitable for the elaboration of specific research imaging techniques. This makes the real time RF signal essential for future algorithms and tools development in ultrasound research. This approach offers the opportunity for medical imaging laboratories to access real time ultrasound RF signal, to implement their own signal processing techniques and develop new imaging modalities. The availability of the normal functions of the scanner while recording RF data makes possible comparative studies, the research team being able to acquire the signals while the medical team is achieving examinations. The system developed in our own laboratory, and exposed in this document, showed that the implementation of the PIP on the RF signals rather than the B mode image is indeed improving the resolution of the system and allows a fair localization. The real time needle localization system aimed by our research is made possible to implement with increased resolution. Such an approach has benefits for both technical studies and teaching, and renewing older engines that are still efficient for research needs.

ACKNOWLEDGEMENTS

This work was supported by the Fonds d'Incitation au Transfert de Technologie, EZUS, Université Lyon 1.

REFERENCES

1. Dydenko, N. Rognin, F. Jamal, C. Cachard, D. Friboulet. Contrast Agent Detection Based on Autoregressive Spectral Estimation. WCU Paris, pp. 193–196, 2003.
2. J. A. Jensen. A Model for the Propagation and Scattering of Ultrasound in Tissue. *J Acoust Soc Am*, vol. 89, N° 1, pp. 182–191, 1991.
3. J. Ophir, I. Céspedes, H. Ponnekanti, Y. Yazdi, X. Li. Elastography: A Quantitative Method for Imaging the Elasticity of Biological Tissues. *Ultrason Imaging* 13, pp. 111–134, 1991.
4. E. Brusseau, J. Fromageau, N. Rognin, P. Delachartre, D. Vray. Local Estimation of RF Ultrasound Signal Compression for Axial Strain Imaging: Theoretical Development and Experimental Results. *IEEE Eng Med Biol Mag*, pp. 86–94, 2002.
5. J. Bercoff, M. Tanter, S. Chaffai, M. Fink. Ultrafast Imaging of Shear Waves Induced by Acoustic Radiation-Force in Soft Tissues. 1st International Conference on the Ultrasonic Measurement and Imaging of Tissue Elasticity, Niagara Falls, Canada, 2002.
6. M. Arditi, T. Bernier, M. Schneider. Preliminary study in differential contrast echography, Ultrasound in Medicine and Biology. *Ultrasound Med Biol*, 23(8), 1185–1194, 1997.
7. W. G. Wilkening, J. H. Lazenby, H. Ermert. A method for detecting echoes from microbubble contrast agents based on time-variance. *Biomedical Application*, 1998.
8. J. M. Mari. Ultrasonic localization of strongly scattering inclusions in soft tissues, application to electrode detection. PhD thesis, 152 pages, Claude Bernard University Lyon 1, France, December 2004.
9. M. Barva, J. M. Mari, J. Kybic, C. Cachard. A Radial Radon Transform dedicated to Micro-object Localization from Radio Frequency Ultrasound Signal. *IEEE Ultrasonic Symposium*, Montreal, Canada, 2004.
10. M. Barva, J. M. Mari, J. Kybic, C. Cachard. Automatic localization of curvilinear object in 3D ultrasound images. *Biomedical Engineering*, Czech Technical University, Czech Republic, SPIE, 2005.
11. M. Berson, L. Vaillant, F. Patat, L. Pourcelot. High-resolution real-time ultrasonic scanner. *Ultrasound Med Biol*, vol 18, N° 5, pp 471–478, 1992.
12. S. Foster, M. Zhang, Y. Zhou, G. Liu, J. Mehi, E. Cherin, K. Harasiewicz, B. Starkoski, L. Zan, D. Knapik, L. Adamson. A new ultrasound instrument for in vivo microimaging. *Ultrasound Med Biol*, vol. 28, pp. 1165–1172, 2002.
13. L. Masotti, E. Biagi, M. Calzolari, L. Capineri, S. Granchi, M. Scabia. FEMMINA: a Fast Echographic Multiparametric Multi Imaging Novel Apparatus. *IEEE Ultrasonics Symposium*, pp. 739–748, 1999.
14. E. Biagi, M. Calzolari, M. Forzieri, S. Granchi, L. Masotti, M. Salerno, M. Scabia, M. Scortecci. Real Time Processing of the Radiofrequency Ultrasonic Echo Signal for on Line Spectral Maps. *Proc. of the 24th International Symposium Acoustical Imaging*, vol. 24, New York: Kluwer Academic / Plenum Press, 1998, pp. 95–100. 1998.
15. J. A. Jensen, O. Holm, L. Joost, H. Bendsen, S. Ivanov et al. Ultrasound Research Scanner for Real-time Synthetic Aperture Image Acquisition. *IEEE Trans Med Imaging*, vol. 22, N°1, 2003.
16. K. Thomenius. Evolution of ultrasound beamformers. *IEEE Ultrasonic Symposium*, pp. 1615–1622, 1996.
17. N. Rognin, C. Mérel, C. Cachard, E. Brusseau, G. Finet. Ultrasound Contrast Agent in Intravascular Echography: Parametric Mapping Based on RF Output. *IEEE Ultrasonic Symposium*, pp. 1787–1790, 2000.